Dynamic pathways to mediate reactions buried in thermal fluctuations. II. Numerical illustrations using a model system

Shinnosuke Kawai[1,a)] and Tamiki Komatsuzaki[1,2]
[1]*Molecule and Life Nonlinear Sciences Laboratory, Research Institute for Electronic Science, Hokkaido University, Kita 20 Nishi 10, Kita-ku, Sapporo 001-0020, Japan*
[2]*Core Research for Evolutional Science and Technology (CREST), Japan Science and Technology Agency (JST), Kawaguchi, Saitama 332-0012, Japan*

(Received 6 October 2009; accepted 6 November 2009; published online 9 December 2009)

The framework recently developed for the extraction of a dynamic reaction coordinate to mediate reactions buried in thermal fluctuation is examined with a model system. Numerical simulations are carried out for an underdamped Langevin equation with the Müller–Brown potential surface, which contains three wells and two saddles, and are compared to the prediction by the theory. Reaction probabilities for specific initial conditions of the system as well as their average over the Boltzmann distribution are investigated in the position space and in a space spanned by the position coordinates and the velocities of the system. The nonlinear couplings between the reactive and the nonreactive modes are shown to have significant effects on the reactivity in the model system. The magnitude and the direction of the nonlinear effect are different for the two saddles, which is found to be correctly reproduced by our theory. The whole position-velocity space of the model system is found to be divided into the two distinct regions: One is of mainly reactive (with reaction probability more than half) initial conditions and the other, the mainly nonreactive (with reaction probability less than half) ones. Our theory can actually assign their boundaries as the zero of the statistical average of the new reaction coordinate as an analytical functional of both the original position coordinates and velocities of the system (solute), as well as of the random force and the friction constants from the environment (solvent). The result validates the statement in the previous paper that the sign of the reaction coordinate thus extracted determines the fate of the reaction. Physical interpretation of the reactivity under thermal fluctuation that is naturally derived, thanks to the analyticity of the theoretical framework, is also exemplified for the model system. © *2009 American Institute of Physics*. [doi:10.1063/1.3268622]

I. INTRODUCTION

Chemical reactions in condensed phase are subject to the effect of their environment with thermal fluctuations. The environment plays a pivotal role both to make the system to surmount and cross through the "barrier" of the reaction (i.e., energy activation), and also to deactivate the excited system to settle down in either the product or the reactant by failure of the reaction (i.e., energy dissipation). In the pioneering works by Kramers[1] and by Grote and Hynes,[2] they represented condensed phase reactions under thermal fluctuation in terms of Langevin and generalized Langevin equations. The reactions are represented as a motion along a single coordinate, the so-called reaction coordinate, feeling the potential of mean force and the random force with the friction constant or friction kernel (incorporating the memory effect on that coordinate) arisen from the surrounding environment. The system-bath Hamiltonian approach can formally bridge the descriptions of *any* Hamiltonian system and the generalized Langevin formulation projected onto a chosen coordinate.[3–5] However, the question of what reaction coordinate the system *actually* follows in a thermally fluctuating environment still remains. Here, we use the term "reaction coordinate" as a single one-dimensional coordinate that can describe the progress of the reaction without referring to the other coordinates so that it can, *in principle*, predict the destination of the reaction, that is, reactants or products.

van der Zwan and Hynes[5] and later Pollak[6] showed in the harmonic bath Hamiltonian systems that the reaction rate of the Grote–Hynes formulation with an arbitrarily chosen reaction coordinate is exactly equivalent to that of the transition state theory if one chooses a reaction coordinate as an unstable normal coordinate of the total system (=system +bath). This reaction coordinate was decoupled from the rest, free from the recrossing problem, and can *a priori* identify the destination of the reaction at any instant solely by the value of that reaction coordinate. This indicates that the appropriate coordinate to mediate the reaction may have to involve all the coordinates of the system and the thermal bath because they are mutually coupled, in general.[7]

In the previous paper,[8] we have presented a formulation for analyzing nonlinear dynamics of chemical reactions in the region of saddle in condensed phase. We adopted the description of the reaction system by multidimensional underdamped Langevin equation without any assumption for the form of the potential of mean force. The theory explicitly takes into account nonlinearities of the (reacting) system and their couplings with the surrounding environment via friction

[a)]Electronic mail: skawai@es.hokudai.ac.jp.

constants and fluctuating, stochastic random force. It was shown that under certain conditions, a coordinate transformation can be performed to give a new coordinate to mediate reaction that is decoupled from all the other coordinates, as a nonlinear functional of the original coordinates and velocities of the system and the random force with the friction constants. The sign of the new reaction coordinate in the region of saddle can predict the fate of the reaction, that is, whether the trajectory will proceed to the product by overcoming the barrier or be carried back to the reactant.

In this article, in order to demonstrate the potential of the theory, we analyze nonlinear reaction dynamics of underdamped Langevin equation of a model system. We scrutinize how the theory can provide us with means to address the question of what determines the destination of the reaction in a thermally fluctuating environment.

II. THEORY

We present a brief summary of the theory we developed in the previous paper.[8] Chemical reactions in condensed phase are described by a multidimensional Langevin equation,

$$\ddot{\boldsymbol{q}} = -\frac{\partial U}{\partial \boldsymbol{q}} - \gamma \dot{\boldsymbol{q}} + \boldsymbol{\xi}(t), \tag{1}$$

where $\boldsymbol{q}$ is the normal mode position coordinates of the system (solute), U is the potential (of the mean force), γ is the friction constant, and $\boldsymbol{\xi}(t)$ describes the random force from the solvent. Although the theory is applicable to systems of any dimensions, we illustrate the theory with a specific example of the Müller–Brown potential[9] (See Sec. III) as U, for which case we have two position coordinates $\boldsymbol{q}=(q_1,q_2)$. The trajectory calculation is performed[10] with the random force sampled according to the fluctuation-dissipation theorem,

$$\langle \boldsymbol{\xi}(t)\boldsymbol{\xi}(0)^{\mathrm{T}}\rangle = 2k_{\mathrm{B}}T\gamma\delta(t), \tag{2}$$

where $\boldsymbol{\xi}(0)^{\mathrm{T}}$ is the transpose of the vector $\boldsymbol{\xi}(0)$, T is the temperature, and k_{B} is the Boltzmann constant. The force from the potential U can be expanded in a Taylor series,

$$-\frac{\partial U}{\partial q_j} = -k_j q_j + \sum\nolimits_{|\boldsymbol{m}|\geq 2} \alpha_{j,\boldsymbol{m}} q_1^{m_1} \ldots q_n^{m_n}, \tag{3}$$

with the expansion coefficients k_j and $\alpha_{j,\boldsymbol{m}}$ for the linear and the nonlinear parts, respectively. Here, $|\boldsymbol{m}|=\Sigma_j m_j$ and $\Sigma_{|\boldsymbol{m}|\geq 2}$ sums over combinations of m_j satisfying $|\boldsymbol{m}|\geq 2$.

The theory introduces a nonlinear coordinate transformation that involves both the position (q_1,q_2) and the velocity $(\dot{q}_1,\dot{q}_2)$ to introduce a special coordinate system $\boldsymbol{y}=(y_1,y_2,y_3,y_4)$. The purpose of the transformation is to make the equation of motion into the following form:

$$\dot{y}_1 \approx [\lambda_1 + c_1(t)]y_1, \tag{4}$$

$$\dot{y}_2 \approx \lambda_2 y_2 + c_2(\boldsymbol{y},t), \tag{5}$$

$$\dot{y}_3 \approx \lambda_3 y_3 + c_3(\boldsymbol{y},t), \tag{6}$$

$$\dot{y}_4 \approx \lambda_4 y_4 + c_4(\boldsymbol{y},t). \tag{7}$$

Here $\lambda_1>0$ is a positive real value, $\lambda_2<0$ is a negative real, and λ_3 and λ_4 are complex numbers with a negative real part, conjugate to each other. The coefficient $c_1(t)$ depends only on time and not on the coordinates. The other terms $c_j(\boldsymbol{y},t)$ $(j=2,3,4)$ can take any functional forms. The solution of Eq. (4) is given by

$$y_1(t) = y_1(t_0)\exp\left[\int_{t_0}^{t} (\lambda_1 + c_1(t'))dt'\right], \tag{8}$$

where t_0 is a certain instant of time (the initial condition). If $c_1(t)$ does not exceed λ_1 in magnitude [more precisely, see Eq. (34) of the previous paper[8]], we have $y_1(t)\to\pm\infty$ as $t\to+\infty$. That is, the motion along y_1 is unstable, corresponding to the motion sliding down the barrier of reaction. The direction (the sign) of this motion along y_1 is determined by the initial sign of $y_1(t_0)$ and does not change with time. One can thus predict the fate of the reaction (whether the reaction system proceeds to the product or goes back to the reactant) solely by the sign of y_1 at any instant when it is in the saddle region. This is thanks to the fact that the equation of motion along y_1 does not depend on the other coordinates (y_2,y_3,y_4) in Eq. (4).

The detailed procedure for finding the transformation to make the equation into the form of Eq. (4) is given in the previous paper.[8] The resulting transformation from the original coordinates $(\boldsymbol{q},\dot{\boldsymbol{q}})$ to y_1 is generally expressed in the following form:

$$\begin{aligned} y_1 = {} & a_1 q_1 + a_2 \dot{q}_1 - S[\lambda_1,\tilde{\xi}_1](t) + F_0[\boldsymbol{\xi}](t) \\ & + \sum\nolimits_{|\boldsymbol{m}|\geq 2} w_{\boldsymbol{m}} q_1^{m_1} \ldots q_n^{m_n} \dot{q}_1^{m_{n+1}} \ldots \dot{q}_n^{m_{2n}} \\ & + \sum_{|\boldsymbol{m}|\geq 1} F_{\boldsymbol{m}}[\boldsymbol{\xi}](t) q_1^{m_1} \ldots q_n^{m_n} \dot{q}_1^{m_{n+1}} \ldots \dot{q}_n^{m_{2n}}. \end{aligned} \tag{9}$$

All the coefficients depend on the friction constants, while only $S[\lambda_1,\tilde{\xi}_1](t)$, $F_0[\boldsymbol{\xi}](t)$, and $F_{\boldsymbol{m}}[\boldsymbol{\xi}](t)$ include the random force and are therefore time dependent.

In the previous paper,[8] the physical interpretation of each term appearing in Eq. (9) was also given. Briefly, the first two terms correspond to linear approximation that reflects the harmonic part of the potential and friction constant. The third term $S[\lambda_1,\tilde{\xi}_1](t)$ expresses direct environment effect, that is, the kick by the random force along the reactive normal mode direction. The terms with the coefficients $w_{\boldsymbol{m}}$ come from the nonlinearity of the system (here, nonlinearity means both nonlinear couplings among modes and nonlinearity along each mode's coordinate). The rest terms [with $F_0[\boldsymbol{\xi}](t)$ and $F_{\boldsymbol{m}}[\boldsymbol{\xi}](t)$] are the combined effects of the environment and the nonlinearity, in the sense that they arise only when there exist both the random force and the nonlinearity in the potential. For example, the terms of $F_0[\boldsymbol{\xi}](t)$ tell us how much the vibrational motion along the nonreactive mode changes the reactivity through nonlinear couplings between the nonreactive and the reactive modes when the nonreactive mode is excited by a kick from the environment.

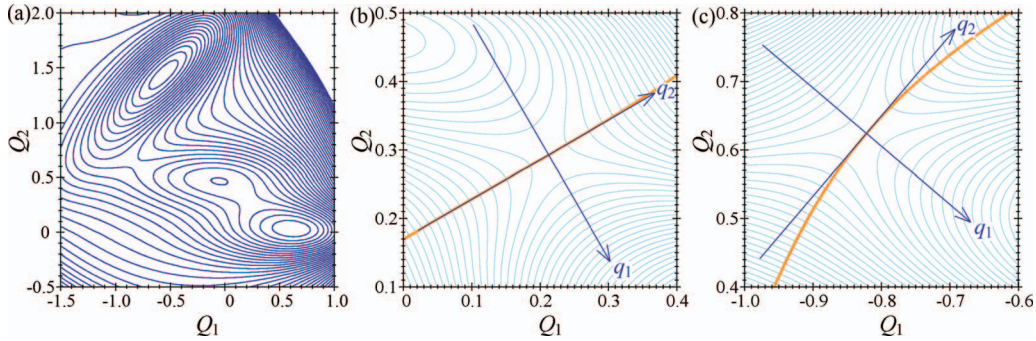

FIG. 1. (a) Contour plot of Müller–Brown potential. The contours are spaced by 10. Magnifications of the potential surface with configuration space normal mode coordinates are shown for the regions of (b) saddle 1 and (c) saddle 2. The contours are spaced by 1. The coordinate q_1 corresponds to the reactive direction, and q_2 is the nonreactive one. The ridge of the potential is shown by bold orange line. For saddle 1, the ridge almost coincides with the q_2 axis.

Those of $F_{\boldsymbol{m}}[\boldsymbol{\xi}](t)$ tell us how much the amplitude of couplings among $(\boldsymbol{q},\dot{\boldsymbol{q}})$ depends on the $\boldsymbol{\xi}(t)$: The random force disturbs the position of the system on the potential, resulting in the change in the coupling strength.

Equation (9) above can be calculated only when one knew the instance of the random force $\boldsymbol{\xi}(t)$ for all the past and the future time in advance. In practice, however, what one may assume *a priori* is the statistical properties of $\boldsymbol{\xi}(t)$ as an ensemble rather than a single instance. In the previous paper,[8] using the statistical properties of random force such as the fluctuation-dissipation theorem, we also analytically formulated the ensemble average of the reaction coordinate y_1 over all realizations of $\boldsymbol{\xi}(t)$,

$$\begin{aligned}\langle y_1\rangle &= a_1 q_1 + a_2 \dot{q}_1 + \bar{F}_0(k_{\mathrm{B}}T)\\ &\quad + \sum_{|\boldsymbol{m}|\geq 2} w_{\boldsymbol{m}} q_1^{m_1}\ldots q_n^{m_n}\dot{q}_1^{m_{n+1}}\ldots \dot{q}_n^{m_{2n}}\\ &\quad + \sum_{|\boldsymbol{m}|\geq 1} \bar{F}_{\boldsymbol{m}}(k_{\mathrm{B}}T) q_1^{m_1}\ldots q_n^{m_n}\dot{q}_1^{m_{n+1}}\ldots \dot{q}_n^{m_{2n}},\end{aligned} \tag{10}$$

where the time-independent coefficients $\bar{F}_0(k_{\mathrm{B}}T)$ and $\bar{F}_{\boldsymbol{m}}(k_{\mathrm{B}}T)$ are the averages of the corresponding terms in Eq. (9) and are functions of temperature through Eq. (2). The direct environment effect vanishes by taking the average of $\boldsymbol{\xi}(t)$.

III. MODEL SYSTEM

As a model system we use the Müller–Brown potential,[9] which has often been used as a test system for searching algorithms of minima and saddle points. The potential U is expressed in terms of two position coordinates (Q_1,Q_2) by

$$\begin{aligned}U(Q_1,Q_2) &= \sum_{i=1}^{4} A_i \exp[a_i(Q_1-Q_{1,i}^0)^2 + b_i(Q_1-Q_{1,i}^0)(Q_2\\ &\quad - Q_{2,i}^0) + c_i(Q_2-Q_{2,i}^0)^2],\end{aligned} \tag{11}$$

with $A=(A_1,A_2,A_3,A_4)=(-200,-100,-170,15)$, $a=(-1,-1,-6.5,0.7)$, $b=(0,0,11,0.6)$, $c=(-10,-10,-6.5,0.7)$, $Q_1^0=(1,0,-0.5,-1)$, and $Q_2^0=(0,0.5,1.5,1)$. The contour plot of the potential is shown in Fig. 1(a). This system possesses three minima and two saddle points. The locations, energies, and normal mode frequencies (without friction) of the stationary points are summarized in Table I. The normal mode frequencies at the two saddles (without friction) simply reflect the curvatures of the potential. The friction constant is set to be proportional to unit matrix $\gamma_{ij}=30\delta_{ij}$. This value was regarded as the underdamped case because it is of the same order with the normal mode frequency of the system.

In the simulation we prepared initial conditions around the saddle points, and then propagated the trajectory until it "settles down" in either of the wells. The propagation was performed by the method proposed by Ermak and Buckholz[10] with the random force sampled according to the fluctuation-dissipation theorem with time step 10^{-3}. As a criterion for the destination of the reaction, the system was judged to have settled down in the well when the energy (defined as the kinetic energy plus the potential) becomes less than $U_{\min}+2k_{\mathrm{B}}T$ after leaving the region of the saddle. Here $U_{\min}$ is the potential at the bottom of each well and $2k_{\mathrm{B}}T$ the average thermal energy of two degrees of freedom

TABLE I. Name, location, energy, and frequencies of the stationary points.

				Normal mode frequencies	
Name	Q_1	Q_2	Energy	Reactive	Nonreactive
Minimum 1	−0.558	1.442	−147		
Minimum 2	0.623	0.028	−108		
Minimum 3	−0.050	0.467	−81		
Saddle 1	0.212	0.293	−72	27.1	22.6
Saddle 2	−0.822	0.624	−40	27.4	22.1

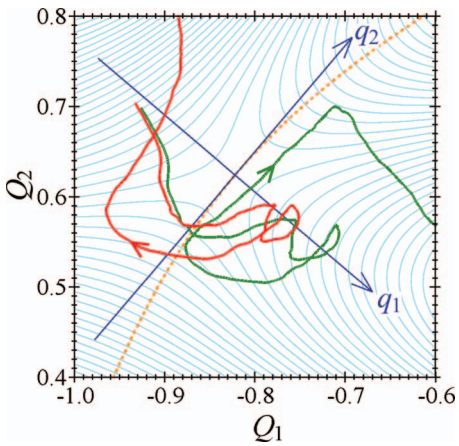

FIG. 2. Examples of trajectories with the effects of friction and random force, shown superimposed with contours of the surface of the potential $U(\boldsymbol{q})$. The configuration space normal mode coordinates (q_1,q_2) are shown. The friction is chosen to be comparable in size with the harmonic frequencies at the saddle point. The temperature is below the barrier height relative to the minima. A reactive trajectory is shown by the green line and a nonreactive trajectory is shown in red. The coordinate q_1 corresponds to the reactive direction and q_2 corresponds to the nonreactive (vibrational) mode. The ridge of the potential is shown by the orange dotted line.

system in thermal bath of temperature T. The smallest energy difference between a saddle and a minimum is that of saddle 1 and minimum 3, which is equal to 9. Therefore, the representation of the system having settled down in either of the wells becomes meaningless unless $k_BT<9/2$ is satisfied.

We introduce position space normal mode coordinates (q_1,q_2) which diagonalize the potential at each saddle point. The directions are shown in Figs. 1(b) and 1(c). We used the same symbol for both saddle points, although the directions are different. Note here that the configuration space normal mode coordinates $\boldsymbol{q}$ are functions of only the position coordinates, and diagonalize the harmonic part of the potential, while the normal mode coordinates $\boldsymbol{u}$ in the position-velocity space defined in Eqs. (7) and (8) in the previous paper are functions of both the position and the velocity, and diagonalize the $2n\times 2n$ matrix consisting of the harmonic potential, the friction, and the kinetic energy.

IV. RESULTS AND DISCUSSION

A. An illustrative example of reactive and nonreactive trajectories

Figure 2 shows two examples of trajectories with the contours of the potential. The green line shows a reactive trajectory that starts on one side of the barrier, which is here defined naïvely as $q_1=0$, passes over it and goes to the other side. The red line is a nonreactive trajectory that crosses the barrier but is reflected back into its original region.

In Fig. 3(a), the same trajectories are plotted in position (q_1) and velocity $(\dot{q}_1)$ along the reactive direction. The velocity fluctuates more significantly than the position due to the random force. The direction of q_1 in the configuration space is shown in Fig. 2. In Fig. 3(a), we also show the normal mode coordinates (u_1,u_2) in the position-velocity space that diagonalize the linear part [see Eqs. (7) and (8) in the previous paper]. The normal mode coordinate u_1 corresponds to the unstable motion sliding down the barrier.

Figure 3(b) shows plots of the two trajectories in the relative coordinates (x_1,x_2) introduced in Sec. IIB in the previous paper. The trajectories have become much smoother than the corresponding plots in Fig. 3(a). This implies that the shift of coordinates[12–14,19] incorporates the effect of the random force to some extent. However, the nonreactive trajectory starts at $x_1>0$, crosses the line $x_1=0$, and finally returns to the left side of the figure. Therefore this line still does not function as the boundary of reaction when significant nonlinearities exist in the potential U.

Figure 3(c) plots the two trajectories in the normal form (NF) coordinates (y_1,y_2) (see Sec. IIC in the previous paper). The coordinates are calculated by partial NF up to the second order perturbation. It is clearly seen that $y_1=0$ separates correctly the reactive and the nonreactive trajectories. This means that the newly introduced reaction coordinate y_1 can tell the reactivity of the system correctly even in the presence of fluctuating environment and nonlinearity.

B. Reaction probabilities

Figure 4 shows the numerical results of reaction probabilities P_{reaction}, for three different temperatures k_BT

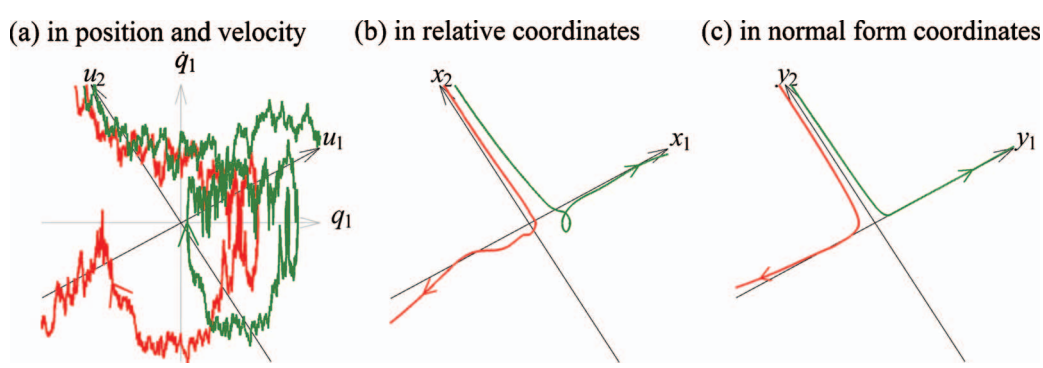

FIG. 3. Examples of trajectories (same as Fig. 2) plotted in three sets of coordinates. (a) Trajectories plotted in the position-velocity space. The normal mode coordinates (u_1,u_2) in the position-velocity space, which diagonalize the linearized equation of motion, are also shown. (b) Trajectories plotted in relative coordinates (x_1,x_2) obtained by subtracting the reference trajectory from (u_1,u_2). The trajectories have become smooth but cross the line $x_1=0$. (c) Trajectories plotted in normal form coordinates (y_1,y_2) obtained through a nonlinear transformation from (x_1,x_2). The coordinates are obtained by second order perturbation to normalize the equation of motion for both y_1 and y_2. The space defined by $y_1=0$ now functions as a boundary that separates the reactive and the nonreactive trajectories.

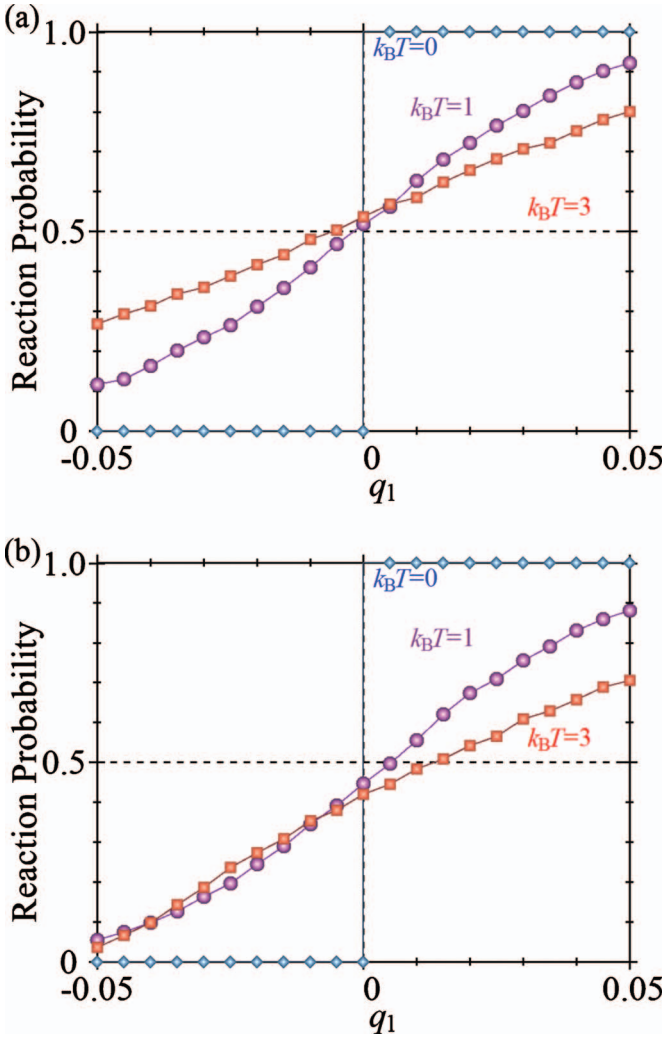

FIG. 4. Reaction probabilities as functions of the normal mode reaction coordinate q_1 for (a) saddle 1 and (b) saddle 2 of the Müller–Brown potential surface. Average is taken for the other coordinates (Boltzmann distribution) and the random force (Gaussian distribution given by dissipation-fluctuation theorem). The temperatures are $k_BT=0$ (diamond), 1 (circle), and 3 (square).

$=0,1,3$, as functions of q_1 (i.e., the reactive normal mode in the coordinate space). The reaction probability for a surface of $q_1=\alpha$ is given by

$$P_{\text{reaction}}(q_1=\alpha) = \frac{\int d\boldsymbol{q}d\dot{\boldsymbol{q}}\,\delta(q_1-\alpha)P(\boldsymbol{q},\dot{\boldsymbol{q}})\exp(-E(\boldsymbol{q},\dot{\boldsymbol{q}})/k_BT)}{\int d\boldsymbol{q}d\dot{\boldsymbol{q}}\,\delta(q_1-\alpha)\exp(-E(\boldsymbol{q},\dot{\boldsymbol{q}})/k_BT)}. \tag{12}$$

We took each surface of constant q_1 on which all the other $(\boldsymbol{q},\dot{\boldsymbol{q}})$ are sampled according to the Boltzmann distribution. Then the trajectory calculation was performed starting from these initial conditions with different instances of random forces $\boldsymbol{\xi}$ satisfying Eq. (2) with the same k_BT. $P(\boldsymbol{q},\dot{\boldsymbol{q}})$ and $E(\boldsymbol{q},\dot{\boldsymbol{q}})$ denote the reaction probability for a given initial condition $(\boldsymbol{q},\dot{\boldsymbol{q}})$ and a sum of the kinetic and the potential energies, respectively,

$$E(\boldsymbol{q},\dot{\boldsymbol{q}}) = (\dot{q}_1^2+\dot{q}_2^2)/2 + U(q_1,q_2). \tag{13}$$

Here $k_BT=0$ corresponds to the situation where there is no random force [Eq. (2)] and no initial excitation along the nonreactive mode. Therefore P_{reaction} is either 0 or 1. The positive side $(q_1>0)$ is reactive and the negative side $(q_1<0)$ is nonreactive. Therefore the halfway point $(P_{\text{reaction}}=1/2)$ at $q_1=0$ can be regarded as the boundary between the reactive and nonreactive initial conditions at zero temperature. As the temperature increases, P_{reaction} takes intermediate values between 0 and 1. This results in broadening of the plot of P_{reaction} in Fig. 4 compared to the steplike behavior at $k_BT=0$. The major origin of this broadening was found to be the fluctuation of the direct solvent effect $S[\lambda_1,\tilde{\xi}_1](t)$ in Eq. (9) for the ensemble of $\tilde{\xi}_1(t)$. In nonzero temperature, the halfway point $P_{\text{reaction}}=1/2$ can also be regarded as a boundary of reaction that divides *the* space (one dimension in this case) into a "mainly reactive" $(P_{\text{reaction}}>1/2)$ region and a "mainly nonreactive" $(P_{\text{reaction}}<1/2)$ one. The boundary is slightly shifted to the negative-q_1 direction for saddle 1 [Fig. 4(a)] and significantly to the positive-q_1 direction for saddle 2 [Fig. 4(b)]. It implies that the normal mode picture q_1 cannot provide us insights about the fate of the reaction (except at zero temperature): In order to identify the location of the reaction boundary that divides the space into mainly reactive and mainly nonreactive regions, one cannot assign without trajectory calculations (unless one has information of y_1 in Sec. II).

Next we show the results of normal form calculations formulated in the previous paper which was applied to the Müller–Brown system. Normal form calculations have been performed up to the second order of perturbation. In Fig. 5, the surface $q_1=0$ is taken and the reaction probability on the surface is plotted against the averaged normal form reaction coordinate y_1. The reaction probability for a surface of $\langle y_1\rangle=\beta$ is given by

$$P_{\text{reaction}}(\langle y_1\rangle=\beta;q_1=0) = \frac{\int d\boldsymbol{q}d\dot{\boldsymbol{q}}\,\delta(q_1)\delta(\langle y_1\rangle-\beta)P(\boldsymbol{q},\dot{\boldsymbol{q}})\exp(-E(\boldsymbol{q},\dot{\boldsymbol{q}})/k_BT)}{\int d\boldsymbol{q}d\dot{\boldsymbol{q}}\,\delta(q_1)\delta(\langle y_1\rangle-\beta)\exp(-E(\boldsymbol{q},\dot{\boldsymbol{q}})/k_BT)}. \tag{14}$$

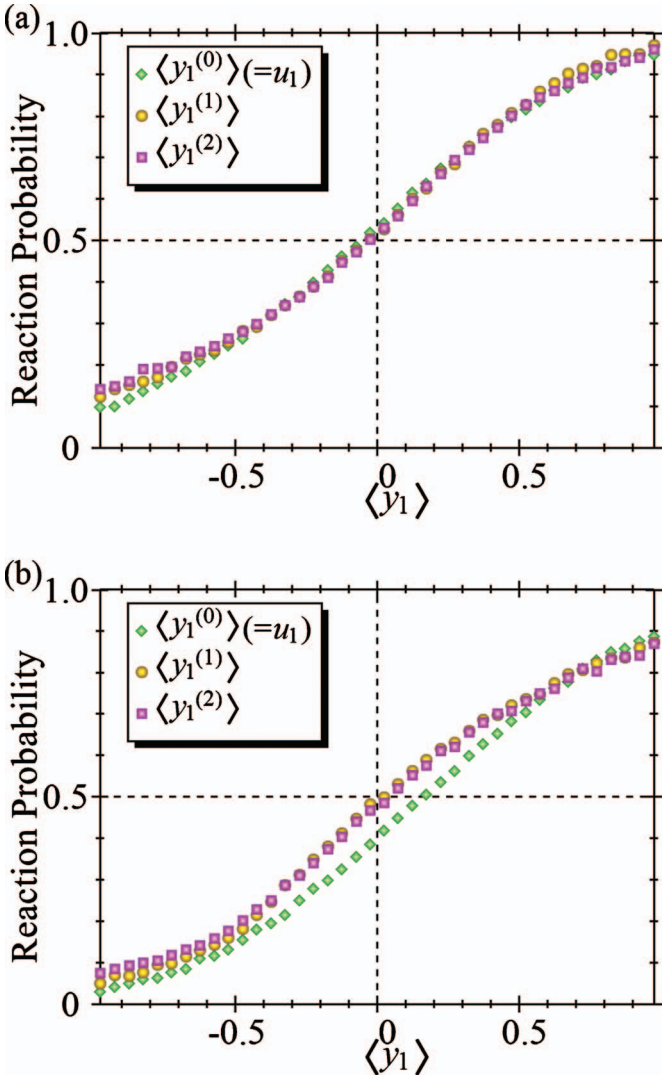

FIG. 5. Reaction probabilities as functions of the averaged normal form reaction coordinate $\langle y_1 \rangle$ for (a) saddle 1 and (b) saddle 2 of the Müller–Brown potential surface. The temperatures is $k_B T=3$. Plots for zeroth, first, and second order perturbations are shown in diamond, circle, and square, respectively.

Here $\langle y_1 \rangle$ is calculated as a function of $(\boldsymbol{q},\dot{\boldsymbol{q}})$ by Eq. (10). In the sampling by the Boltzmann distribution in Eq. (14), the initial conditions for $(\boldsymbol{q},\dot{\boldsymbol{q}})$ except q_1 are "restricted" (or highly populated) near zero in the region of the saddle point except at very high temperature T because the energy of the system E in the Boltzmann factor increases as the size of these variables increases. However, since q_1 is along the unstable direction of the potential, the Boltzmann factor increases the statistical weight for large $|q_1|$ so that expansions such as Eq. (3) cannot be validated. Since our interest in the present paper is the dynamics in the saddle region, we have posed the condition $q_1=0$ into Eq. (14) in order to perform the sampling in the saddle region. Note also that the condition $\langle y_1 \rangle = \beta$ makes no restriction on the $|q_1|$ to small values (e.g., $y_1=0$ forms the unstable manifold emanating from the saddle region; see also Fig. 3). In Fig. 5, we take the same simulation data for $q_1=0$ as used in the numerical simulation of Fig. 4. One can see that as the order of the perturbation increases, the halfway point $P_{\text{reaction}}=1/2$ comes closer to the origin $\langle y_1 \rangle=0$. This shows that the normal form theory correctly gives the location of the boundary of reaction between the mainly reactive region and the mainly nonreactive region even in the presence of thermal fluctuation.

Normal form theory presented in this paper is capable of providing physical insights into the observed behavior of reaction probabilities, as analytical expressions for the reaction coordinate are available. Explicit expressions for the averaged normal form reaction coordinate $\langle y_1 \rangle$ are obtained up to the second order,

$$\begin{aligned}\langle y_1^{(2)} \rangle &= 11.887 q_1 + 0.258 \dot{q}_1 + 0.007 k_B T \\ &\quad + \sum_{2 \le |\boldsymbol{m}| \le 3} w_{\boldsymbol{m}} q_1^{m_1} q_2^{m_2} \dot{q}_1^{m_3} \dot{q}_2^{m_4} (30 \text{ terms}) \\ &\quad + 0.008 k_B T q_1 + 0.002 k_B T \dot{q}_1 - 0.033 k_B T q_2 \\ &\quad + 0.005 k_B T \dot{q}_2 \end{aligned} \tag{15}$$

for saddle 1 and

$$\begin{aligned}\langle y_1^{(2)} \rangle &= 12.041 q_1 + 0.260 \dot{q}_1 - 0.020 k_B T \\ &\quad + \sum_{2 \le |\boldsymbol{m}| \le 3} w_{\boldsymbol{m}} q_1^{m_1} q_2^{m_2} \dot{q}_1^{m_3} \dot{q}_2^{m_4} (30 \text{ terms}) \\ &\quad + 0.087 k_B T q_1 + 0.002 k_B T \dot{q}_1 + 0.015 k_B T q_2 \\ &\quad - 0.001 k_B T \dot{q}_2 \end{aligned} \tag{16}$$

for saddle 2, where the terms are aligned in the same order as Eq. (10). (The full expressions of $\langle y_1 \rangle$ including the numerical values of $w_{\boldsymbol{m}}$ and also the normal form reaction coordinate y_1 before taking the ensemble average of random force are available online in supplementary material of this paper[11]). In the right hand side of each equation, the first two terms linear in q_1 and $\dot{q}_1$ with constant coefficients come from the linear approximation [Eq. (8) in the previous paper]. The third term originating from $F_0[\boldsymbol{\xi}](t)$ makes the shift of the coordinate origin observed in Fig. 4 (see below). The last four terms linear (at least up to second order) in $\boldsymbol{q}$ and $\dot{\boldsymbol{q}}$ with temperature-dependent coefficients originate from the environment-mediated coupling effect of $F_{\boldsymbol{m}}[\boldsymbol{\xi}](t)$: The force from the environment $[\boldsymbol{\xi}(t),\boldsymbol{\gamma}]$ disturbs the position of the system on the landscape of potential U, resulting in the change in the coupling strength.

To begin, let us briefly look into the "structure" of these expressions. As first indicated by Van der Zwan and Hynes,[5] the coordinate to mediate the reaction involves all the coordinates and velocities of the system and the thermal bath. The appearance of q_2 and $\dot{q}_2$ is the effect of nonlinear couplings because they mean that the excitation along the nonreactive mode influences the reaction. There are only linear terms in $\boldsymbol{q}$ and $\dot{\boldsymbol{q}}$ for the environment-mediated coupling effect $[\bar{F}_{\boldsymbol{m}}(k_B T)]$, while the polynomial with the coefficients $w_{\boldsymbol{m}}$ is cubic. This is due to the truncation in Eqs. (15) and (16) at the second order perturbation $[O(\varepsilon^2)]$. Note that the order assignment is such that the element $S[\lambda_j,\tilde{\xi}_j](t)$ is of $O(\varepsilon)$ [see Eqs. (11) and (12) in the previous paper]. We have temperature-dependent coefficients in the third term and the last four terms, corresponding to $\bar{F}_0(k_B T)$ and $\bar{F}_{\boldsymbol{m}}(k_B T)$ in Eq. (10), respectively. They arise from convolutions or products of $S[\nu,\xi_j](t)$ such as $\langle S[\nu_3, S[\nu_1,\xi_i] S[\nu_2,\xi_j]] \rangle$ and

$\langle S[\nu_1,\xi_i]S[\nu_2,\xi_j]\rangle$. The numbers ν_i are combinations of λ_j as in Eq. (26) of the previous paper.[8] Before taking the ensemble average of $\boldsymbol{\xi}(t)$, $F_0[\boldsymbol{\xi}](t)$ and $F_{\boldsymbol{m}}[\boldsymbol{\xi}](t)$ contain 355 and 612 terms, respectively.[11] It was also found that the more the friction constant γ increases, the more the contributions of velocities $\dot{\boldsymbol{q}}$ in y_1 and $\langle y_1\rangle$ tends to decrease in magnitude (see the supplementary material available online of this paper[11]). This provides us with the firm basis to address the questions of what size of frictions make the effect of moment of inertia negligible.

Let us turn to the following question: "What is the primary driving force to make the reaction boundary $P_{\text{reaction}}=1/2$ migrate?" In Fig. 4 it was found that the direction of the migration of the boundary is to $q_1<0$ for saddle 1 and $q_1>0$ for saddle 2. The amount of the shift is larger for saddle 2 than that for saddle 1, and it increases when temperature T increases. In fact, simple observation of the third term in Eqs. (15) and (16) already tells some feature of the shift, because it increases with temperature, has opposite sign for the two saddles and its absolute value is larger for saddle 2 than saddle 1. The interpretation for the shift for the case of $(q_2,\dot{q}_1,\dot{q}_2)|_{t=0}=(0,0,0)$ is given as follows: From Eqs. (15) and (16),

$$\langle y_1^{(2)}\rangle = 0.007k_{\mathrm{B}}T + (11.887 + 0.008k_{\mathrm{B}}T)q_1 + O(q_1^2)$$

for saddle 1 and

$$\langle y_1^{(2)}\rangle = -0.020k_{\mathrm{B}}T + (12.041 + 0.087k_{\mathrm{B}}T)q_1 + O(q_1^2)$$

for saddle 2. This implies that in the vicinity of $q_1=0$, $\langle y_1\rangle \approx \bar{F}_0+(a_1+\bar{F}_{\boldsymbol{m}'})q_1$ ($\bar{F}_{\boldsymbol{m}'}$ is the coefficient of q_1 in environment-mediated coupling terms). Then, q_1 at the reaction boundary of $P_{\text{reaction}}=1/2$, where $\langle y_1\rangle=0$ is given by $q_1\approx-\bar{F}_0/a_1$ since a_1 arises from the linear approximation which is much larger than the $\bar{F}_{\boldsymbol{m}'}$. Namely, the primary driving force to shift the reaction boundary outward from $q_1=0$ mainly originates from $\bar{F}_0$. The sign of $\bar{F}_0$ depends on the nonlinear couplings between the reactive q_1 and nonreactive mode q_2 in the region of the saddle.

By comparing the term $\bar{F}_0[k_{\mathrm{B}}T]$ with the corresponding terms $F_0[\boldsymbol{\xi}](t)$ before taking the average,[11] we can see that this term comes from terms of the following types:

$$S[\nu_1,\xi_1]S[\nu_2,\xi_1],\quad S[S[\nu_1,\xi_1]S[\nu_2,\xi_1]],$$

$$S[\nu_1,\xi_2]S[\nu_2,\xi_2],\quad S[S[\nu_1,\xi_2]S[\nu_2,\xi_2]], \tag{17}$$

with ν_1,ν_2 being some constants. Note that terms like $\langle S[\nu_1,\xi_1]S[\nu_2,\xi_2]\rangle$ do not contribute to $\bar{F}_0[k_{\mathrm{B}}T]$ because in this paper, we use uniform friction $\gamma_{12}=0$. The contribution can be evaluated quantitatively for each term. For saddle 2, we have found that 77% of contribution is from ξ_2, whereas 76% is from ξ_1 for saddle 1. Since ξ_2 is the random force along the direction of the nonreactive mode, the interpretation for saddle 2 is as follows: The nonreactive mode vibration is first excited by the kick from the solvent. The ridge of the potential surface around saddle 2 [Fig. 1(c)] has a curved shape toward the positive direction of q_1. Hence, as the nonreactive vibrational mode is excited, the effective position of the barrier along the reactive direction shifts toward the positive side.

Due to the order assignment in the theory [see Eqs. (11) and (12) in the previous paper], all the terms in Eq. (17) are assigned $O(\varepsilon)$. Therefore the shift of the origin for the case of $(q_2,\dot{q}_1,\dot{q}_2)|_{t=0}=(0,0,0)$ is accounted for by the first order perturbation. In fact, the increase in the order to the second order does not improve the situation very much [see Figs. 5(a) and 5(b)]. The initial condition of $(q_2,\dot{q}_1,\dot{q}_2)|_{t=0}=(0,0,0)$ is of course one example and the physical interpretation of which terms dominate a shift (whenever it exists) in q_1 depends on the initial condition.

One of the striking consequences of our theory is this: such "two-step" scenario of direct nonreactive mode excitation by the solvent followed by interaction of the nonreactive mode with the reactive mode can be called "combined effect" of the solvent and the nonlinearity inside the solute. By the direct excitation of the nonreactive mode, we mean the transition state trajectory [Eq. (11) in the previous paper] introduced by Bartch *et al.*[12–14] In their theory, however, the coupling among the normal modes were ignored so that the motion along the normal mode reactive coordinate was independent of the nonreactive modes. Under the existence of coupling, however, the excitation of the nonreactive mode can affect the reaction through the nonlinear coupling between the reactive and the nonreactive modes. Our theory here is capable of handling such general nonlinear cases.

We have stated that the coefficient $c_1(t)$ appearing in the equation of motion of y_1 [Eq. (4)] must not exceed λ_1 in magnitude in order that the sign of y_1 determines the fate of the reaction. Here we check the condition in the present numerical example by calculating the mean and variance of $c_1(t)$. For saddle 1 and $k_{\mathrm{B}}T=3$, it gives

$$\lambda_1 = 15.988,\quad \langle c_1(t)\rangle = -2.594,$$

$$\langle (c_1(t)-\langle c_1(t)\rangle)^2\rangle^{1/2} = 4.778, \tag{18}$$

and for saddle 2 with the same temperature,

$$\lambda_1 = 16.239,\quad \langle c_1(t)\rangle = -0.449,$$

$$\langle (c_1(t)-\langle c_1(t)\rangle)^2\rangle^{1/2} = 5.560. \tag{19}$$

Thus it is confirmed that $c_1(t)$ is smaller than λ_1 at least on average.

C. Dynamical dividing surfaces buried in a thermal fluctuation

Figure 6 shows the reaction probability at saddle 2 as a function of nonreactive normal mode coordinates $(q_2,\dot{q}_2)|_{t=0}$ by the gradation of color. There the initial conditions for the reactive mode is fixed to $q_1|_{t=0}=0$, and $\dot{q}_1|_{t=0}=0.1$, 0.3, and 0.5, for (a), (b), and (c), respectively. The dependence of the reaction probability on the nonreactive mode, seen as the nonuniformity in the plot, is a consequence of the nonlinear coupling between the reactive and the nonreactive modes. Although the probability is not 0 or 1 due to the stochastic nature of the random force, we can still find a distinction between mainly reactive region (that with lighter colors), and mainly nonreactive region (with darker colors).

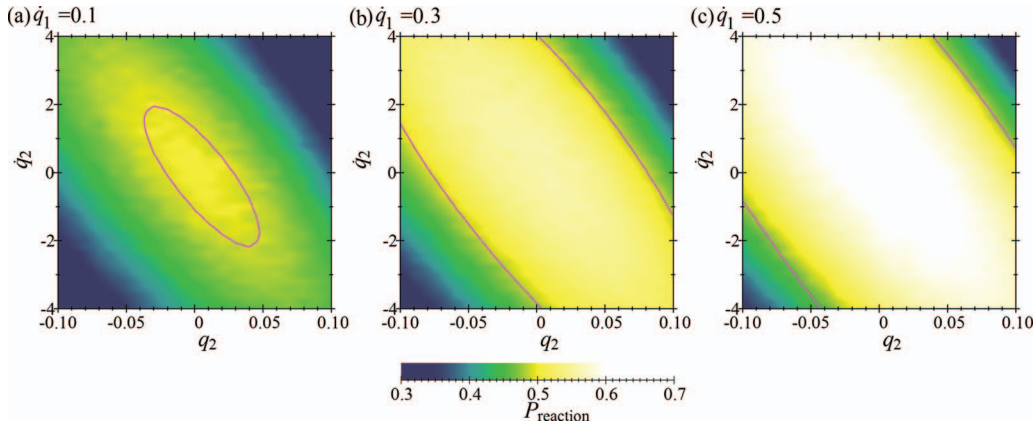

FIG. 6. Reaction probability as a function of nonreactive mode coordinates $(q_2,\dot{q}_2)$ at $t=0$ obtained from numerical simulations with $k_BT=1$ at saddle 2. The initial values for the reactive mode are fixed to $q_1|_{t=0}=0$ and $\dot{q}_1|_{t=0}=0.1$, 0.3, and 0.5, for (a), (b), and (c), respectively. Purple line is given by $\langle y_1\rangle=0$ calculated by second order normal form. It is seen that the line locates the boundary between the mainly reactive and the mainly nonreactive regions.

The purple line in Fig. 6 is given by $\langle y_1\rangle=0$ from the second order normal form calculation, which can be obtained as an analytical function of $\boldsymbol{q}$ and $\dot{\boldsymbol{q}}$ of the system without performing any trajectory calculation. For $\dot{q}_1|_{t=0}=0.1$, the mainly reactive region is small centered around the origin. As $\dot{q}_1$ increases, the region becomes larger and the probability at the center also increases. In all the cases, the line given by $\langle y_1\rangle=0$ correctly separates the mainly reactive and the mainly nonreactive regions.

In Fig. 7, we further add one dimension of the plot, i.e., $\dot{q}_1$. The other coordinate, q_1, takes the same value as Fig. 6. Three semitransparent surfaces show the section of the surface $\langle y_1\rangle=0$ for $k_BT=0,1,3$. The yellow horizontal plane is given by $\dot{q}_1=0.3$ and therefore corresponds to the plot in Fig. 6(b). Basically, the system has more reaction probability for larger positive value of the velocity $\dot{q}_1$ along the reactive mode. Thus the upper part of the figure is more reactive than the lower. However, the border between the mainly reactive and the mainly nonreactive regions shows dependence on q_2, $\dot{q}_2$, and the temperature.

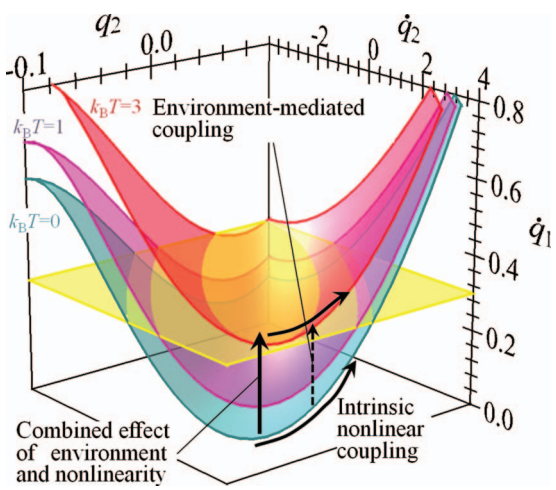

FIG. 7. Surfaces obtained by $\langle y_1\rangle=0$ on the three-dimensional section of $q_1|_{t=0}=0$ at saddle 2. Blue, purple, and red semitransparent surfaces are $\langle y_1\rangle=0$ for $k_BT=0,1,3$, respectively. The yellow plane shows the plane given by $\dot{q}_1=0.3$ corresponding to panel (b) of Fig. 6. Physical interpretations for the shapes of the surfaces are also shown.

By such plots, one can visually capture the physical interpretations given in the preceding paragraphs. Here the physical origins of the shapes of the surfaces are schematically superimposed in Fig. 7. All the three surfaces are curved in contrast to a plane of $\dot{q}_1$=const, implying that reactivities at each temperature depend on the nonreactive mode $(q_2,\dot{q}_2)$. This curved shape is interpreted as it primarily arises from the intrinsic nonlinear couplings of the system (i.e., the terms with $w_{\boldsymbol{m}}$) because the dependence of reactivity exists even at $k_BT=0$. The surface shifts upward in the direction of $\dot{q}_1$ as the temperature increases. The shift along $\dot{q}_1$ can be explained in a similar way with that along q_1 given in Sec. IV B. Note that the shift exists even at $(q_2,\dot{q}_2)=\mathbf{0}$ and we fix $q_1=0$ in Fig. 7. In this case, at least from small $\dot{q}_1$, we have $\langle y_1\rangle\approx\bar{F}_0(k_BT)+a_2\dot{q}_1$. The reaction boundary $\langle y_1\rangle=0$ can then be given by $\dot{q}_1\approx-\bar{F}_0(k_BT)/a_2$. Thus the primary reason for the shift of the boundary surface with the temperature is the temperature dependence of $\bar{F}_0(k_BT)$, whose physical origin is the effect of the random force from the environment combined with the nonlinearity of the system, as has been explained in Sec. IV B. If the nonreactive mode $(q_2,\dot{q}_2)$ has nonzero values, the position of the reaction boundary changes due to the terms with $w_{\boldsymbol{m}}$ and $\bar{F}_{\boldsymbol{m}}(k_BT)$ in Eq. (10). Then, due to the temperature dependence of $\bar{F}_{\boldsymbol{m}}(k_BT)$, the shape (i.e., gradients, curvature, etc.) of the surface also changes with temperature rather than a parallel translation. In other words, the extent of the nonlinear couplings among the modes $(\boldsymbol{q},\dot{\boldsymbol{q}})$ depend on the temperature, and therefore the change in the shape of the boundary surface can be interpreted as the environment-mediated coupling.

V. SUMMARY AND OUTLOOK

We demonstrated the potential of the framework we developed recently for the analyses of condensed phase chemical reactions. We used the Müller–Brown potential,[9] which has distinct two saddles with three minima, as an illustrative example. Along the same direction recently established in many degrees of freedom, Hamiltonian systems that extract a new reaction coordinate decoupled from the other (nonreactive) coordinates from the phase space (one can see several

reviews[7,15–21] and books[22,23]), our theory extracts a reaction coordinate (called y_1 in this paper) at least in the region of rank-one saddle, decoupled from the other (nonreactive) coordinates, from the reaction system even when it is embedded in a thermally fluctuating environment. The numerical simulations showed that reactive and nonreactive trajectories are separated by the boundary $y_1=0$, in which the nonlinearity and the solvent effects are explicitly taken into account. Even though taking the statistics of the fluctuating random force disables the unique determination of the fate of the reaction to some extent, the average position of the boundary ($\langle y_1 \rangle = 0$) remains robustly to provide a dynamical structure to separate the mainly reactive and mainly nonreactive regions in the position-velocity space of the system.

The analytical expression of y_1 in terms of the positions and the velocities before transformation provides a way of analyzing the physical origin of the reactivity. In particular, the numerical simulation in this paper showed an example of combined effects of the solvent and the nonlinearity: "effective barrier shift" that was caused by the vibrational excitation of the nonreactive mode by the kick from the environment, followed by the nonlinear interaction between the nonreactive and the reactive modes.

In the preceding paper, we discussed the possible resonance mechanism to break down the existence of y_1, which makes reaction totally unpredictable (i.e., the birth of "full stochasticity" in reactions). In the model system with chosen temperatures and friction constants in this paper, we have not met such situation up to the order we considered.

Given, for instance, any specific value or a distribution of initial conditions in the barrier region (e.g., Ref. 24), our framework enables us to analytically calculate the probability distributions of y_1 (hence the reaction probability). For example, the linear shift [type (ii) in our classification] is zero on average but contributes to the fluctuation, whereas the terms second order in the random force [type (iv)] has nonzero average. These physical insights can help us to understand what type of specific, initial distribution should be prepared in the region of saddle, so as to lead us to a desired product. We believe that our theory can provide us with physical insights to control chemical reactions in a fluctuating media, although several things remain to be considered such as quantum effects.[20,25] It is also expected to shed light on the mechanism of why biological (nonlinear) systems can robustly perform their functions under unpredictable, stochastic thermal fluctuation.

ACKNOWLEDGMENTS

This work was supported by the Research Fellowships of the Japan Society for the Promotion of Science for Young Scientists (to S.K.) and by JSPS, JST/CREST, Priority Area "Molecular Theory for Real Systems" (to T.K.). S.K. is a research fellow of the Japan Society for the Promotion of Science.

[1] H. A. Kramers, Physica (Amsterdam) **7**, 284 (1940).
[2] R. F. Grote and J. T. Hynes, J. Chem. Phys. **73**, 2715 (1980).
[3] H. Mori, Prog. Theor. Phys. **33**, 423 (1965).
[4] R. Zwanzig, Phys. Rev. **124**, 983 (1961).
[5] G. van der Zwan and J. T. Hynes, J. Chem. Phys. **78**, 4174 (1983).
[6] E. Pollak, Chem. Phys. Lett. **127**, 178 (1986).
[7] T. Komatsuzaki and R. S. Berry, Adv. Chem. Phys. **130**, 143 (2005).
[8] S. Kawai and T. Komatsuzaki, J. Chem. Phys. **131**, 224505 (2009).
[9] K. Müller and L. D. Brown, Theor. Chim. Acta **53**, 75 (1979).
[10] D. L. Ermak and H. Buckholz, J. Comput. Phys. **35**, 169 (1980).
[11] See EPAPS supplementary material at http://dx.doi.org/10.1063/1.3268622 for the full expressions of the reaction coordinate y_1 in terms of $(\boldsymbol{q},\dot{\boldsymbol{q}})$.
[12] T. Bartsch, R. Hernandez, and T. Uzer, Phys. Rev. Lett. **95**, 058301 (2005).
[13] T. Bartsch, T. Uzer, and R. Hernandez, J. Chem. Phys. **123**, 204102 (2005).
[14] T. Bartsch, T. Uzer, J. M. Moix, and R. Hernandez, J. Chem. Phys. **124**, 244310 (2006).
[15] T. Komatsuzaki and R. S. Berry, Adv. Chem. Phys. **123**, 79 (2002).
[16] M. Toda, Adv. Chem. Phys. **123**, 153 (2002).
[17] C. Jaffé, S. Kawai, J. Palacián, P. Yanguas, and T. Uzer, Adv. Chem. Phys. **130**, 171 (2005).
[18] M. Toda, Adv. Chem. Phys. **130**, 337 (2005).
[19] T. Bartsch, J. M. Moix, R. Hernandez, S. Kawai, and T. Uzer, Adv. Chem. Phys. **140**, 191 (2008).
[20] H. Waalkens, R. Schubert, and S. Wiggins, Nonlinearity **21**, R1 (2008).
[21] S. Kawai, H. Teramoto, C.-B. Li, T. Komatsuzaki, and M. Toda, "Dynamical reaction theory based on geometric structures in phase space," Adv. Chem. Phys. (in press).
[22] *Geometrical Structures of Phase Space in Multidimensional Chaos: Applications to Chemical Reaction Dynamics in Complex Systems*, Advances in Chemical Physics, edited by M. Toda, T. Komatsuzaki, T. Konishi, R. S. Berry, and S. A. Rice (John Wiley & Sons, Hoboken, NJ, 2005), Vol. 130A (and references therein).
[23] *Kinetics and Nonlinear Dynamics of Complex Many Body Systems*, Advances in Chemical Physics, edited by R. S. Berry, T. Komatsuzaki, and D. M. Leitner (John Wiley & Sons, Hoboken, NJ, in press).
[24] J. C. Polanyi and A. H. Zewail, Acc. Chem. Res. **28**, 119 (1995).
[25] D. Schuch, Int. J. Quantum Chem. **72**, 537 (1999).